Theory of the electronic states and absorption spectrum of the LiCl:Ag^+ impurity system

Koblar A. Jackson* and Chun C. Lin
Department of Physics, University of Wisconsin, Madison, Wisconsin 53706
(Received 24 July 1989)

The impurity absorption spectra of Ag^+ and Cu^+ impurities in alkali halide hosts show characteristically different features, despite the similar nature of the corresponding free ions. We use the self-interaction-corrected local-spin-density (SIC-LSD) theory to calculate the electronic structure of the ground state ($4d$) and the $5s$ and $5p$ excited states of the LiCl:Ag^+ impurity ion. The method of linear combinations of atomic orbitals is used to determine the wave functions and energy levels. By comparing with previous calculations for LiCl:Cu^+, we are able to attribute the differences in the $d \rightarrow s$ and $d \rightarrow p$ transitions in the ultraviolet spectra of these systems to the increased bonding between host crystal and impurity orbitals in LiCl:Ag^+, due to the more extensive nature of the Ag^+ $4d$ orbitals. A modification of the earlier SIC-LSD impurity-crystal procedure is introduced to treat the strongly mixed impurity states.

I. INTRODUCTION

The convenience of the Hohenberg-Kohn-Sham local-spin-density theory (LSD) for calculating the properties of many-atom systems has made it a cornerstone of modern computational condensed-matter physics. In LSD, the total energy of an N-electron system is calculated from a simple functional of the electronic charge density,[1-3] using no adjustable parameters. By calculating this energy as a function of nuclear coordinates, the structural properties of multiatom systems are computed, in most cases yielding results in very good agreement with experiment.[4] As a one-electron theory, however, LSD proves less reliable. The eigenvalues of the LSD effective Hamiltonian, H^{LSD}, are commonly interpreted as electron-removal energies, yet in the simple case of the free atom LSD eigenvalues poorly describe electron ionization energies. Furthermore, in energy-band calculations, where the eigenvalues are taken as band energies, semiconductor and insulator band gaps are commonly underestimated by 50% or more. In recent years it has been recognized that the failure of the one-electron aspects of LSD, specifically the correspondence of one-electron eigenvalues in LSD to removal energies, is due to the presence of a residual self-interaction of the electrons in H^{LSD}. The self-interaction correction (SIC) to LSD has been formulated[5] by Perdew and Zunger to address this problem. In SIC-LSD, an additional term is added to the LSD energy functional to explicitly remove the electronic self-interaction. With the self-interaction effects removed, the SIC-LSD eigenvalues become good approximations to electron-removal energies. Atomic ionization energies, for example, are given very accurately in SIC-LSD,[5,6] and insulator band gaps have been calculated in good agreement with experiment.[7,8]

Localized crystal impurities represent a class of problems for which SIC-LSD is particularly well suited and for which LSD is particularly ill suited. The proper placement of impurity energy levels relative to the host-crystal energy bands is essential to understanding the electronic structure of these systems. This requires both the reasonable representation of the host-crystal energy bands, in particular the band gap, and the correct rendering of the atomiclike impurity levels. A computationally convenient SIC-LSD approach has recently been used to study the Cu^+ substitutional impurity in three different alkali halide systems,[9-11] as well as the F center in LiF.[12] In this method an embedded cluster scheme is used in which the impurity-state wave functions are represented by a linear combination of atomic orbitals (LCAO) basis set within a cluster, while the entire impurity crystal contributes to the Hamiltonian. The results of these calculations for impurity-related transition energies have been in good agreement with corresponding experimental measurements.

In this work we study the LiCl:Ag^+ system. The Ag^+ impurity differs significantly from the Cu^+ impurity studied previously because of the more extensive nature of the Ag^+ orbitals: the outermost occupied Ag^+ $4d$ orbitals have considerable overlap with the nearest-neighbor Cl^- ions (the ligands). This overlap significantly strengthens the influence of the host crystal on the impurity ion, and changes dramatically the nature of the impurity states, in contrast to Cu^+ systems where the occupied states associated with the defect ion were highly localized on the defect site, undergoing only slight mixing with the ligand orbitals. Consequently, the treatment of the SIC potential for the impurity problem originally formulated for the Cu^+ systems with atomiclike impurity states[9] must be modified for application to LiCl:Ag^+. We use the general SIC-LSD formalism to derive a new approach for the Ag^+ system, taking into account the strong mixing of the impurity and ligand orbitals. In this new method we treat the host valence band and the Ag^+4d orbitals together in applying the SIC. This generalizes in practice past SIC calculations which were based on bands deriving

essentially from the states associated with a single atomic species.

In Sec. II we give a brief overview of the SIC-LSD formalism, referring the reader to earlier works for further details concerning the general theory. In Sec. III we present the results of our calculation, comparing them with corresponding experimental observations.[13,14] Section IV is a discussion of the SIC-LSD results for LiCl:Ag^+, with detailed comparisons made to the earlier Cu^+ calculations and to the results of a previous calculation on LiCl:Ag^+ using a different technique. We conclude in Sec. V with comments about this and related work.

II. SIC-LSD THEORY

A. Ground-state properties

The SIC-LSD theory[5] is based on the total-energy functional $E_t^{\text{SIC-LSD}}$, which comprises the standard LSD total energy, E_t^{LSD}, and the self-interaction correction, U^{SIC}:

$$E_t^{\text{SIC-LSD}}=E_t^{\text{LSD}}+U^{\text{SIC}} . \tag{1}$$

For an N-electron system with total-electron density ρ and spin densities $\rho_\uparrow$ and $\rho_\downarrow$ the LSD energy is written[2]

$$E_t^{\text{LSD}}=T+U_{\text{ext}}+\tfrac{1}{2}\int d\mathbf{r}\int d\mathbf{r}'\,\frac{\rho(\mathbf{r})\rho(\mathbf{r}')}{|\mathbf{r}-\mathbf{r}'|} -\tfrac{3}{4}(6/\pi)^{1/3}\sum_\sigma\int d\mathbf{r}[\rho_\sigma(\mathbf{r})]^{4/3} . \tag{2}$$

Here, T is the kinetic energy and U_{ext} the external interaction energy (due to the nuclei). The next two terms are the Coulomb and exchange-correlation energies, respectively. The Kohn-Sham exchange-only form[2] for the exchange-correlation energy functional is used here to illustrate the theory; an additional correlation functional may be appended to this expression to explicitly represent electronic correlation effects. This is a straightforward extension of the theory and will not be discussed further in this section.

Expressing ρ in terms of single-electron orbitals $\phi_{i\sigma}$ and orbital densities $\rho_{i\sigma}$ as

$$\rho=\sum_{i,\sigma}\rho_{i\sigma}=\sum_{i,\sigma}|\phi_{i\sigma}(\mathbf{r})|^2 , \tag{3}$$

and rewriting the electronic Coulomb energy in terms of these orbitals, it is easily seen that the Coulomb energy contains contributions from each of the orbitals interacting with itself. This self-Coulomb interaction is only partly canceled by a corresponding self-exchange interaction of the electrons in the exchange energy [the fourth terms of Eq. (2)]. Thus in Eq. (1) we introduce U^{SIC} to remove exactly the self-Coulomb and approximately the self-exchange energy of the electrons from E_t^{LSD}:

$$U^{\text{SIC}}=-\sum_{i,\sigma}\left\{\tfrac{1}{2}\int d\mathbf{r}\int d\mathbf{r}'\,\frac{\rho_{i\sigma}(\mathbf{r})\rho_{i\sigma}(\mathbf{r}')}{|\mathbf{r}-\mathbf{r}'|} -\tfrac{3}{4}(6/\pi)^{1/3}\int d\mathbf{r}[\rho_{i\sigma}(\mathbf{r})]^{4/3}\right\} . \tag{4}$$

Self-consistent-field (SCF) equations are derived for the orbitals in the usual way by seeking an extremum for $E_t^{\text{SIC-LSD}}$ through variations of the ϕ's:

$$H_{i\sigma}^{\text{SIC-LSD}}\phi_{i\sigma}=(H_\sigma^{\text{LSD}}+V_{i\sigma}^{\text{SIC}})\phi_{i\sigma}=\sum_j\lambda_{ij}^\sigma\phi_{j\sigma} , \tag{5}$$

where

$$H_\sigma^{\text{LSD}}=-\tfrac{1}{2}\nabla^2+V_{\text{ext}}+\int d\mathbf{r}'\,\frac{\rho_\sigma(\mathbf{r}')}{|\mathbf{r}-\mathbf{r}'|} -(6/\pi)^{1/3}[\rho_\sigma(\mathbf{r})]^{1/3} , \tag{6}$$

$$V_{i\sigma}^{\text{SIC}}=-\int d\mathbf{r}'\,\frac{\rho_{i\sigma}(\mathbf{r}')}{|\mathbf{r}-\mathbf{r}'|} +(6/\pi)^{1/3}[\rho_{i\sigma}(\mathbf{r})]^{1/3} , \tag{7}$$

and λ_{ij} are the Lagrange multipliers (LM). Equation (7) indicates that the SIC potential for an orbital i is the negative of the self-interaction (Coulomb and exchange) potential for the corresponding orbital density ρ_i.

The last two equations illustrate an important difference between SIC-LSD and the parent LSD theory. While the effective Hamiltonian in LSD, H_σ^{LSD}, depends only on the total spin density, ρ_σ, the SIC-LSD Hamiltonians, $H_{i\sigma}^{\text{SIC-LSD}}$, depend on the orbital densities, $\rho_{i\sigma}$. This orbital dependence is linked to the correction term U^{SIC}, which is not a functional of the total spin densities only, but rather depends on the individual orbital densities. Because of this orbital dependence the variational treatment of the SIC-LSD energy yields an additional set of constraint equations for the orbitals:

$$\langle\phi_{i\sigma}|V_{i\sigma}^{\text{SIC}}-V_{j\sigma}^{\text{SIC}}|\phi_{j\sigma}\rangle=0 . \tag{8}$$

This point has been discussed extensively by Pederson *et al.*[15] Because of the self-Coulomb terms, U^{SIC} is generally more negative for orbitals that are well localized. For this reason, the orbitals satisfying Eqs. (5) and (8) are referred to as the local orbitals (LO); similarly, Eq. (8) is known as the localization equation (LE).

For applications to multiatom systems, Eq. (5) is not the most convenient form for the SCF equations. For these systems, it is computationally expedient to reexpress the SCF equations in terms of functions reflecting the symmetry of the system under study.[15] To do this, we write the LO in terms of a set of orbitals of the proper symmetry via a unitary transformation, M:

$$\phi_{i\sigma}=\sum_j M_{ij}^\sigma\psi_{j\sigma} . \tag{9}$$

Carrying out the variation of $E_t^{\text{SIC-LSD}}$ with respect to the ψ's yields

$$(H_\sigma^{\text{LSD}}+\Delta V_{i\sigma}^{\text{SIC}})\psi_{i\sigma}=\sum_j\lambda_{ij}'^\sigma\psi_{j\sigma} , \tag{10}$$

where

$$\Delta V_{i\sigma}^{\mathrm{SIC}}\psi_{i\sigma}=\sum_j (M_{ij}^{\sigma})^* V_{j\sigma}^{\mathrm{SIC}}\phi_{j\sigma} \ . \tag{11}$$

We call attention to the use of the symbol ΔV^{SIC} to distinguish the SIC potential for the ψ orbitals from V^{SIC}, the SIC potential for the LO (ϕ). There exists a particular choice for the transformation M which diagonalizes the LM matrix, λ'_{ij}, in Eq. (10). The corresponding orbitals are known as the canonical orbitals (CO).[16] In this paper we use the symbol ϕ to refer to the LO, or some approximation to them, while we reserve ψ for the CO or an approximation to them. A good approximation to the CO results when the transformation M removes all the nondiagonal λ'_{ij}'s except those for which $|\lambda'_{ij}| \ll |\lambda'_{ii}-\lambda'_{jj}|$.

The orbital dependence of the SCF equations complicates their solution. In particular, care must be taken to insure the orthogonality of the orbitals associated with different Hamiltonians. To solve this set of equations, we use projection operators P_i to combine the individual $H_{i\sigma}^{\mathrm{SIC}}$ into a single, unified Hamiltonian H_u,[6]

$$H_u=\sum_{i=1}^{N}(P_iH_iP_i+OH_iP_i+P_iH_iO) \ , \tag{12}$$

where

$$P_ig(\mathbf{r})=\phi_i(\mathbf{r})\left[\int d\mathbf{r}'\,\phi_i(\mathbf{r}')g(\mathbf{r}')\right] \ , \tag{13}$$

and

$$O=1-\sum_{i=1}^{N}P_i \ . \tag{14}$$

The spin index has been dropped from the preceding equations to simplify the notation. It is easily shown that the eigenvalue equation for H_u,

$$H_u\psi_i=\varepsilon_i\psi_i \ , \tag{15}$$

is equivalent to Eq. (10) at self-consistency, with the eigenvalue ε_i identified with the diagonal Lagrange multiplier λ'_{ii}.

The orbital energies ε_i corresponding to the SIC-LSD CO have been shown in several previous papers[5,6,16] to be good approximations to electron ionization energies. This feature of SIC-LSD is exploited in a computationally convenient method for calculating energies for single-electron transitions. Consider for an N-electron system the transition $\{N-1\}\phi_a\rightarrow\{N-1\}\phi_b$, where a and b are localized states and $\{N-1\}$ represents the passive orbitals not taking part in the transition. The ground-state unoccupied-orbital approximation (GSUO) (Ref. 6) uses the identification of the SIC-LSD eigenvalues with electron ionization energies to write the transition energy $\Delta E(a\rightarrow b)$ as a simple eigenvalue difference:

$$\Delta E(a\rightarrow b)=\varepsilon_b-\varepsilon_a \ , \tag{16}$$

where

$$\varepsilon_a=\langle\phi_a|(H^{\mathrm{LSD}}+V_a^{\mathrm{SIC}})|\phi_a\rangle \tag{17}$$

and

$$\varepsilon_b=\langle\phi_b|(H^{\mathrm{LSD}}+V_a^{\mathrm{SIC}})|\phi_b\rangle \ . \tag{18}$$

Note the use of the SIC potential for the lower (hole) orbital, V_a^{SIC}, to determine the eigenvalue ε_b for the excited orbital. This procedure has a clear-cut physical motivation: since V_a^{SIC} represents the self-interaction of the electron ϕ_a, $H_a=H^{\mathrm{LSD}}+V_a^{\mathrm{SIC}}$ embodies the interaction of an electron with the external field (i.e., the nuclei) and all the electrons except ϕ_a. This is precisely what electron ϕ_b physically sees in the (unrelaxed) excited configuration. From a practical point of view, the use of H_a in Eq. (18) implies that all the excited orbitals see the same Hamiltonian, and that all the transition energies may be obtained from a single SCF calculation, making the GSUO method computationally very efficient. A second computational advantage is that the transition energy ΔE is of the same order of magnitude as the eigenvalues ε_a and ε_b. This relieves the burdensome constraint of extreme accuracy required to determine the transition energy as the difference in total energies which are several orders of magnitude larger. The GSUO method has been used in various calculations, giving results in each case in good agreement with experiment.

To include the excited states in the unified Hamiltonian formalism presented above, we append an additional term to H_u:[6]

$$H_u=\sum_{i=1}^{N}(P_iH_iP_i+OH_iP_i+P_iH_iO)+OH_{\mathrm{exc}}O \ , \tag{19}$$

where H_{exc} is the SIC-LSD Hamiltonian of the appropriate hole orbital. The eigenvalue equation for H_u [Eq. (15)] is solved self-consistently, and the transition energies are calculated from the eigenvalues via Eq. (16).

B. Application of SIC-LSD to the impurity problem

The embedded cluster, LCAO approach which we apply to the problem of a singly charged substitutional impurity in an alkali halide crystal was formulated by Heaton, Harrison, and Lin,[9] and has been discussed in that work and in our previous paper on the NaCl:Cu^+ system.[10] We present here an outline of the method, referring the interested reader to the cited references.

From spectroscopic data,[13] the Ag^+ ion is known to be an on-site replacement for the like-charged Li^+ ion in the host crystal. This substitution results in a disturbance of the host crystal confined to the vicinity of the impurity site. We represent the local perturbation of the pure-crystal charge, ρ_{PC}, by writing

$$\rho_{\mathrm{IC}}=\rho_{\mathrm{PC}}+\delta\rho \ , \tag{20}$$

where ρ_{IC} is the impurity-crystal charge and $\delta\rho$ is the localized difference charge induced by the impurity. Since the LSD one-electron Hamiltonian depends only on the density ρ_{IC}, it can be written in a similar form:

$$H_{\mathrm{IC}}^{\mathrm{LSD}}=H_{\mathrm{PC}}^{\mathrm{LSD}}+\delta V^{\mathrm{LSD}} \ , \tag{21}$$

where $H_{\mathrm{IC}}^{\mathrm{LSD}}$ and $H_{\mathrm{PC}}^{\mathrm{LSD}}$ are, respectively, the impurity- and pure-crystal one-electron Hamiltonians, and δV^{LSD} is

a localized difference potential. δV^{LSD} consists of a nuclear term, due to the difference in nuclear charge ΔZ between the impurity ion and the alkali ion that it replaces, and Coulomb and exchange terms, arising from the difference in electronic charge density around the impurity site:

$$\delta V^{\mathrm{LSD}}=-(\Delta Z/r)+\int d\mathbf{r}'\,\frac{\delta\rho(\mathbf{r}')}{|\mathbf{r}-\mathbf{r}'|} -(6/\pi)^{1/3}\{[\rho_{\mathrm{IC}}(\mathbf{r})]^{1/3}-[\rho_{\mathrm{PC}}(\mathbf{r})]^{1/3}\}\ . \tag{22}$$

Here we neglect lattice relaxation which we discuss in Sec. IV B.

The application of SIC to a multiatom system depends on the identification of appropriate LO on which to base the SIC potentials V^{SIC} and ΔV^{SIC}. In the case of the impurity, it is useful to discuss the treatment of the states associated with the host crystal and those associated with the impurity ion separately. SIC potentials for the host-crystal states in the impurity-crystal system are patterned after their pure-crystal counterparts. For pure ionic crystals, the LO are the atomiclike Wannier functions (WF), which satisfy Eq. (8) by symmetry. The pure-crystal CO are the Bloch functions, $\psi_{n\mathbf{k}}$, indexed by a band label (n) and crystal momentum ($\mathbf{k}$). Heaton and Lin[7] derived an approximate form of ΔV^{SIC} which may be used for all the ψ's for a given band of the pure crystal:

$$\Delta V_n^{\mathrm{SIC}}(\mathbf{r})=\frac{\sum_{\nu} V_n^{\mathrm{SIC}}(\mathbf{r}-\mathbf{R}_\nu)\eta_n(\mathbf{r}-\mathbf{R}_\nu)}{\sum_{\nu}\eta_n(\mathbf{r}-\mathbf{R}_\nu)}\ . \tag{23}$$

Here, $\eta_n(\mathbf{r})$ is the Wannier density for the nth band, and $V_n^{\mathrm{SIC}}(\mathbf{r})$ is the corresponding local SIC potential [Eq. (7)]. The lattice sum covers the cation or anion sites, respectively, for bands corresponding to cation or anion states. It is convenient to use approximate Wannier densities in Eq. (23). For the core bands, the approximate WF are essentially identical to the corresponding free-ion core orbitals. Because there is no spatial overlap of the core Wannier densities centered on different lattice sites, ΔV^{SIC} for these state reduces to the corresponding free ion V^{SIC} inside each unit cell and the core band SIC potentials can therefore be obtained by translating the free ion V^{SIC} in a given unit cell throughout the crystal. Approximate Wannier densities for the valence band may be obtained using expressions derived in Refs. 7 or 8. These can then be used in Eq. (23) to find the valence-band (VB) SIC potential.

In the substitutional impurity, the appropriate LO are the generalized Wannier functions (GWF).[9,17] Because the translational symmetry of the pure crystal is disrupted by the presence of the impurity ion, the GWF are site dependent; it has been shown, however, that the GWF approach the form of the host-crystal WF exponentially with increasing distance from the impurity.[17] In practice, we have found that the GWF differ significantly from the corresponding host-crystal WF only on the nearest-neighbor shell of ions around the impurity site, i.e., the ligand ions, and then only for the GWF corresponding to the VB orbitals. We may therefore adopt the use of the pure crystal $\Delta V_n^{\mathrm{SIC}}$ potentials for the states associated with the host crystal, except for the $\Delta V_{VB}^{\mathrm{SIC}}$, for which we define a difference potential,

$$(\Delta V_{\mathrm{VB}}^{\mathrm{SIC}})_{\mathrm{IC}}=(\Delta V_{\mathrm{VB}}^{\mathrm{SIC}})_{\mathrm{PC}}+\delta V_{\mathrm{VB}}^{\mathrm{SIC}}\ . \tag{24}$$

This difference may be calculated in a straightforward way by using the pure-crystal approximate WF densities, and the impurity-crystal approximate GWF densities in Eq. (23).

For the states associated with the impurity ion, the LCAO expansion of their wave functions, ψ_{imp}, consists of a major component centered on the impurity site (site 0) mixed with orbitals of the host crystal. In the case of the Cu^+ impurity, the admixture of the host-crystal orbitals amounts to only a few percent of the charge. Thus the site-0 GWF can be well approximated by ψ_{imp}. This step, however, is not valid for LiCl:Ag^+ because the Ag^+ $4d$ impurity states have a much larger component of ligand orbitals. Formally the GWF for the impurity site corresponding to the Ag^+ $4d$ states are to be obtained from the impurity eigenstates via the transformation of Eq. (9), where the ψ's are the states of what can be thought of as the composite Ag^+ $4d$–Cl^- $3p$ band. Approximate Ag^+ $4d$ GWF densities may be found from the states of the composite band using the formalism described by Heaton *et al.*;[9] however, we find that the resulting density coincides very nearly with the free-ion Ag^+ $4d$ orbital. For convenience we use the free-ion orbital as the approximate site-0 GWF. The approximate GWF corresponding to the ligand $3p$ orbitals may also be obtained using the techniques of Ref. 9, but here, too, the approximate GWF density is found to be very similar to the correspond pure-crystal LO density, and we use the latter to approximate the ligand $3p$ GWF. ΔV^{SIC} potentials may now be defined for the states of the composite Ag^+ $4d$–Cl^- $3p$ band. The impurity $4d$ states (see below) are almost entirely ($\sim$98%) localized on the impurity site and the ligand shell. These states have a majority Ag^+ $4d$ character, but with significant ligand-shell components. We use Eq. (23) to define a $\Delta V_{4d}^{\mathrm{SIC}}$ potential which is comparably localized:

$$\Delta V_{4d}^{\mathrm{SIC}}=\frac{1}{\rho_T}\left[\bar{\rho}_{4d}V_{4d}^{\mathrm{SIC}}+\sum_{\mu}^{1\,\mathrm{NN}}\bar{\rho}_{3d}(\mathbf{r}-\mathbf{R}_\mu)V_{3p}^{\mathrm{SIC}}(\mathbf{r}-\mathbf{R}_\mu)\right], \tag{25}$$

where

$$\rho_T(\mathbf{r})=\bar{\rho}_{4d}(\mathbf{r})+\sum_{\mu}^{1\,\mathrm{NN}}\bar{\rho}_{3p}(\mathbf{r}-\mathbf{R}_\mu)\ . \tag{26}$$

$\bar{\rho}_{4d}$ and $\bar{\rho}_{3p}$ are, respectively, free-atom Ag^+ $4d$ and Cl^- $3p$ orbital densities averaged over the m sublevels and V_{4d}^{SIC} and V_{3p}^{SIC} are the corresponding local SIC potentials. The sum on μ extends over the sites of the ligand shell of the first nearest neighbors (1NN).

The remaining states in the composite Ag^+ $4d$–Cl^- $3p$ valence band extend throughout the impurity cluster, including nonzero density on the Ag^+ site. For these states we use Eq. (23) to construct a composite potential $\Delta V_{\mathrm{VB}}^{\mathrm{SIC}}$

which extends throughout the cluster:

$$\Delta V_{\mathrm{VB}}^{\mathrm{SIC}}=\frac{1}{\rho_T}\left[\bar{\rho}_{4d}V_{4d}^{\mathrm{SIC}}+\sum_{\nu}\bar{\rho}_{3d}(\mathbf{r}-\mathbf{R}_\nu)V_{3p}^{\mathrm{SIC}}(\mathbf{r}-\mathbf{R}_\nu)\right]. \tag{27}$$

This potential is similar in form to the $4d$ potential given above, however now the sum on ν extends over all the anion sites in the cluster. Similarly, ρ_T in this equation represents the sum of the $4d$ local-orbital density plus the density of the VB local orbitals centered on all the anion sites of the cluster.

In our LCAO treatment of the impurity problem, we solve the full infinite crystal Hamiltonians, made up of $H_{\mathrm{IC}}^{\mathrm{LSD}}$ and the appropriate SIC potentials, in a finite cluster basis, extending out to the seventh-nearest-neighbor shell in the host crystal [(2,2,0) in units of the nearest-neighbor distance]. The LCAO basis is made up of atomic orbitals corresponding to the occupied states of the impurity, alkali, and halide ions, centered on the respective ion sites in the cluster. Atomic orbitals corresponding to the lowest unoccupied impurity-ion s and p states are also included on the impurity site. The atomic orbitals are expansions of Gaussian-type orbitals, the coefficients of which are determined in free-ion calculations. In addition to these atomic orbitals, single Gaussian orbitals (SGO's) are used on the sites near the impurity to enhance the variational freedom of the basis set. At the Ag^+ site, we used the exponents 1.75478, 0.757801, and 0.355237 in s-, p-, and d-type SGO's, and additionally 0.04145 for s- and p-type SGO's. For the ligand (first-nearest-neighbor) shell, we used the common exponents 0.950083, 0.448205, and 0.159272 for s- and p-type SGO's, plus an s-type with 0.07500, and a p-type with 2.61988. On the nearest Li^+ shell the SGO's 0.997212 and 0.44462 for s- and p-type, and an additional s-type SGO with exponent 0.14012 were used. Finally for the second Cl^- shell we used 0.950083 and 0.448205 for both s- and p-type SGO's plus an s-type with exponent 0.159272 and a p-type with 2.61988. Such a basis leaves a "cushion" of ion shells at the outer edge of the cluster with no variational freedom. This procedure has been shown[18,9] to properly embed the cluster in the pure crystal. The LCAO solutions for the impurity states are linear combinations of the functions in the cluster basis, and we refer to the coefficients in these expansions as the LCAO eigenvectors.

The starting point for the self-consistent calculation is taken from the respective free-ion and pure-crystal calculations. The initial impurity-crystal density is obtained by directly substituting the impurity free-ion charge for the alkali ion charge at a lattice site. The alkali charge is taken from a constrained curve fit of the pure-crystal SCF charge density, the constraint insuring that the fit reflects the ionic nature of the crystal. The various localized potentials defined in Eqs. (22) and (24) are tabulated on a mesh of points centered on the impurity site and extending beyond the first-nearest-neighbor shell of atoms. These potentials are curve fitted to Gaussian-type functions, so that matrix elements in our Gaussian orbital basis set may then be evaluated analytically. The unified Hamiltonian is constructed, and the impurity-crystal eigenstates found. In subsequent iterations the difference potentials are determined directly from the difference in the impurity-crystal charge density obtained from the impurity eigenstates and the pure-crystal charge. The unified Hamiltonian solution is iterated to self-consistency.

To prepare for the LiCl:Ag^+ calculation, we performed a SIC-LSD calculation for LiCl, using the pure-crystal ΔV^{SIC} potentials defined above. The pure-crystal band gap at self-consistency was found to be 11.1 eV, which compares to 5.8 eV using uncorrected LSD, and to an experimental gap of 9.4 eV.[19] The use of SIC is seen to improve the LSD description of the LiCl band structure. We note that the use of SIC-LSD calculations with correlation functionals have given band gaps in still better agreement with experiment than our result above, which was obtained using the Kohn-Sham exchange-only version of the theory. We do not address here the question of which correlation functional is most appropriate for general use. For our purposes the Kohn-Sham exchange-only theory has given very good results for localized transitions in the free Ag^+ ion: using the GSUO procedure we found 5.50 and 10.5 eV for the $4d\rightarrow 5s$ and $4d\rightarrow 5p$ transition energies, respectively, in good agreement with the corresponding experimental results of 5.37 and 10.8 eV.[20] Since we shall be interested in comparisons between the free-ion and impurity-crystal transitions, we adopt the use of the exchange-only version of the theory in the impurity calculation for consistency.

III. RESULTS FOR LiCl:Ag^+

Our discussion of the SIC-LSD results for LiCl:Ag^+ below focuses on the impurity states associated with the Ag^+ ion. Although the direct correspondence of the impurity Ag^+ states to the analogous free-ion states is clouded due to strong mixing of the Ag^+ orbitals with host-crystal states, we find it convenient to continue to speak of impurity Ag^+ $4d$, $5s$, and $5p$ states. These states are defined in detail below. In the O_h point-group symmetry of the host crystal, the Ag^+ $4d$ states are split into doubly degenerate $4de_g$ states and triply degenerate $4dt_{2g}$ states; we use this notation below. The LCAO basis functions from a given ion shell are symmetrized according to the O_h point group in order to block diagonalize the Hamiltonian matrix.

A portion of the LiCl:Ag^+ one-electron eigenvalue spectrum is shown in Fig. 1, with the positions of the pure-crystal valence and conduction bands indicated for reference. Two important features distinguish the impurity system spectrum from the host-crystal band structure: states appearing in the gap between the pure-crystal valence and conduction bands, and a number of energy levels splitting off above and below the host crystal VB. The states split off from the VB are identified by their LCAO eigenvectors as bonding and antibonding mixtures of ligand valence orbitals and Ag^+ $4d$ or $5s$ atomic orbitals. The bonding combinations are lower in energy and shifted down out of the VB, whereas the antibonding combinations are pushed up out of the VB. The states ly-

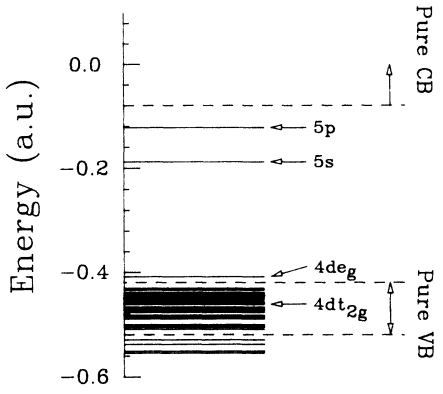

FIG. 1. Calculated energy levels of the 4*d*, 5*s*, and 5*p* impurity states, and the host-crystal valence-band states of LiCl:Ag^+. The ranges of the pure-crystal valence band (VB) and conduction band (CB) are indicated.

ing in the band gap are identified as distorted Ag^+ 5*s* and 5*p* states, extending beyond the impurity site over the first few shell of host-crystal ions.

Closer examination of the LCAO eigenvectors for the split-off states shows the antibonding states to be largely Ag^+ 4*d*-like, although the Cl^- 3*p* components are quite significant. As indicated in Fig. 1, we refer to these levels as impurity Ag^+ 4*d* states. The bonding partners of the Ag^+ 4*d* states have correspondingly less Ag^+ character. (The bonding partners are the unlabeled levels split off slightly from the bottom of the valence band in Fig. 1.) The lowest bonding level has A_{1g} symmetry (corresponding to an *s* state on the impurity site), and is identified as the bonding partner of the antibonding impurity Ag^+ 5*s* state.

The character of the split-off states can be investigated using a Mulliken population analysis[21] of their charge densities. For the Ag^+ $4de_g$ impurity state, 62% of the electron charge is associated with the impurity site, and 36% with the ligand shell. By contrast, 33% and 63% of the charge of the bonding partner to the $4de_g$ state resides on the impurity and the nearest-neighbor shell, respectively. The analysis for the T_{2g} states is similar. The Ag^+ $4dt_{2g}$ state has 73% of its charge on the impurity, and 20% on the ligand shell, while the bonding state has a distribution of 13% and 75%, respectively. The a_{1g} bonding state is largely localized on the ligand shell, with 93% of its charge there, and only a very small amount (0.1%) on the impurity ion site. We note that the impurity 4*d* states are essentially completely localized on the impurity and the ligand shell, consistent with the nature of the SIC potential used for these states.

The first and second lowest-lying excited states in LiCl:Ag^+ consist, respectively, of the Ag^+ 5*s* and 5*p* atomic orbitals mixed with SGO's centered on the impurity sites and the sites of the first few nearest-neighbor shells of host-crystal sites. The Mulliken analysis breaks down for these states because of the large spatial overlap of the SGO's, which contribute heavily to the respective eigenfunctions. Alternatively, we investigate the extent of these states by considering the dependence of their orbital energies on the makeup of the LCAO basis set.[22] As basis functions are removed from the calculation, the quality of the impurity-state representation deteriorates, resulting in higher orbital energies. For reference, we find that removing the SGO's from the basis has no significant effect on the eigenvalues of the occupied states. The impurity $4de_g$ state energy, for example, is −0.390 a.u. with the full basis including SGO's in place. The change in this value due to removing all the SGO's from the cluster basis is 0.0005 a.u., below the convergence criterion for orbital energies used in our calculation (0.001 a.u.). The occupied states are thus seen to be well represented by the atomiclike orbitals in the LCAO basis. By contrast, the energies of the 5*s* and 5*p* states depend strongly on the SGO's. Using the full cluster basis, the 5*s* and 5*p* eigenvalues were −0.16957 and −0.09681 a.u. When the SGO's from the second- and third-nearest-neighbor shells were removed, the eigenvalues were −0.16772 and −0.08618 a.u. Removing the SGO's from the ligand shell gave the values −0.16168 and −0.06879 a.u. Finally, removing the SGO's from the impurity site as well resulted in the energies −0.14959 and −0.02486 a.u. These results indicate that the 5*p* impurity state extends well out to the second- and third-nearest-neighbor shells in the cluster, while the 5*s* is relatively more localized on the impurity site and the ligand shell.

In the GSUO approximation, SIC-LSD transition energies are determined by taking eigenvalue differences [see Eq. (16)]. For the transitions to the lowest-lying impurity excited states, we obtain the results given in Table I, shown along with the corresponding experimental results of LiCl:Ag^+ for comparison. The experimental values shown are the positions of band maxima from the reported LiCl:Ag^+ absorption spectrum. Our results agree quite well with the experimental observations, the two sets differing in the worst case by less than 3%. Note that the difference in the E_g and T_{2g} transitions (1.43 eV) indicates the magnitude of the crystal-field splitting in LiCl:Ag^+, and that the calculated splitting agrees well with experiment (1.25 eV). Of particular note in Table I is the identification of the absorption band at 8.0 eV as the $4de_g \rightarrow 5p$ transition. This assignment is consistent with the suggestion of Pedrini *et al.*[23] The appearance of the $4de_g \rightarrow 5p$ transition of LiCl:Ag^+ at 8 eV is somewhat surprising in that it is only 0.5 eV above the $4d \rightarrow 5s$ manifold of LiCl:Ag^+ but is as much as 2.5 eV below the $4d \rightarrow 5p$ transition energy of the Ag^+ free ion. To contrast this with the Cu^+ impurity we note that the

TABLE I. Theoretical and experimental values of the $4d \rightarrow 5s$ and $4d \rightarrow 5p$ transition energies (in eV) for a free Ag^+ ion and for LiCl:Ag^+.

	Free Ag^+		LiCl:Ag^+	
Transitions	Theor.	Expt.	Theor.	Expt.
$4de_g \rightarrow 5s$	5.50	5.37	6.01	6.17
$4dt_{2g} \rightarrow 5s$	5.50	5.37	7.44	7.42
$4de_g \rightarrow 5p$	10.5	10.8	7.80	7.96

$3de_g \rightarrow 4p$ absorption peak of LiCl:Cu^+ is 1.9 eV above the $3dt_{2g} \rightarrow 4s$ peak and is 1.7 eV below the free-ion $3d \rightarrow 4p$ transition. We discuss the reason for these features in the Ag^+ system in Sec. IV.

The transition energies given in Table I do not account for all of the possible transitions involving states with $4d$ orbital character. We noted above that both the bonding and antibonding combinations of the impurity ion and ligand orbitals in the E_g and T_{2g} representations have sizable Ag^+ $4d$ components. We might therefore expect to see experimental evidence for transitions from both the bonding and antibonding states. Transitions from the bonding states, however, are calculated to occur at energies much larger than 8.6 eV, the exciton edge of the pure LiCl crystal, and would therefore be obscured from measurement by host-crystal absorption.

IV. DISCUSSION

A. Comparison with LiCl:Cu^+

The SIC-LSD results for LiCl:Ag^+ show many of the same features as earlier results obtained for the isovalent systems LiCl:Cu^+ and NaCl:Cu^+.[9,10] In each system, the $nd \rightarrow (n+1)s$ transition ($n=3$ for Cu^+ and $n=4$ for Ag^+) in the impurity crystal requires more energy than the corresponding free-ion transition. Conversely, the impurity $nd \rightarrow (n+1)p$ transition requires less energy than its free-ion counterpart. These are general features of impurity systems of this kind, and are attributed to the bonding or antibonding interaction of the impurity- and host-crystal orbitals.[22] Both the impurity nd and $(n+1)s$ states are antibonding in LiCl:Ag^+ and LiCl:Cu^+; the increase in the impurity $nd \rightarrow (n+1)s$ transition energy arises because the antibonding shift of the impurity $(n+1)s$ level is greater than that of the nd level, due to the greater spatial overlap of the impurity $(n+1)s$ and the ligand $3p$ orbitals. On the other hand, the $nd \rightarrow (n+1)p$ spacing decreases in these systems because the impurity $(n+1)p$ level is the bonding partner to host-crystal CB states, and is shifted down in energy at the same time the antibonding nd levels are shifted up. We show the relationship between impurity and free-ion transitions for both LiCl:Cu^+ and LiCl:Ag^+ graphically in Fig. 2.

We can use the bonding or antibonding picture of impurity transitions to understand the differences between the Ag^+ and Cu^+ impurities seen in Fig. 2. The increase in the $nd \rightarrow (n+1)s$ transition energy for the Ag^+ system over the corresponding free-ion transition is less pronounced than for the Cu^+ system, while at the same time the $nd \rightarrow (n+1)p$ reduction is more pronounced. Focusing first on the $nd \rightarrow (n+1)s$ transition, we note that the Ag^+ $4d$ state has greater spatial extent than the Cu^+ $3d$ state. The $\langle r \rangle$ moment of the Ag^+ $4d$ orbital is 1.38 a.u., versus 1.00 a.u. for Cu^+ $3d$. For reference, the same moment for the Cl^- $3p$ orbital is 2.03 a.u., while for the Ag^+ $5s$ it is 2.81 a.u., and for Cu^+ $4s$ it is 2.46 a.u. The greater extent of the Ag^+ $4d$ orbitals implies greater spatial overlap between the $4d$ and the ligand orbitals, resulting in greater mixing of these orbitals in the impurity

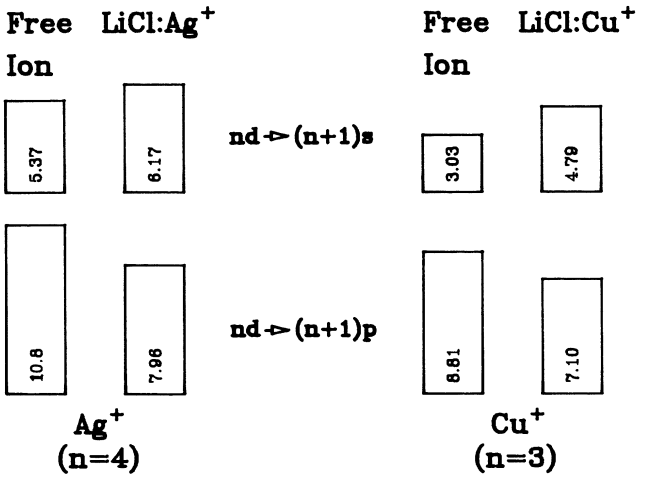

FIG. 2. Comparison of the $nd \rightarrow (n+1)s$ and $nd \rightarrow (n+1)p$ transition energy for the free ions Ag^+ and Cu^+, and the corresponding impurity systems LiCl:Ag^+ and LiCl:Cu^+.

eigenstates compared to the Cu^+ $3d$ orbitals. At the same time, by comparing $\langle r \rangle$ moments above to the LiCl nearest-neighbor spacing of 4.86 a.u, it can be argued that the Cu^+ $4s$ already has significant overlap with the ligand orbitals, so that the difference in spatial extent between the Ag^+ $5s$ and Cu^+ $4s$ is not expected to result in a great difference in the antibonding shift of these states. The net effect is thus to relatively lessen the antibonding difference between the Ag^+ impurity $4d$ and $5s$ states, bringing the $nd \rightarrow (n+1)s$ transition closer to the free-ion value in LiCl:Ag^+ than in LiCl:Cu^+.

As for the $nd \rightarrow (n+1)p$ transition, the free-ion Ag^+ $5p$ orbital has greater spatial extent than the Cu^+ $4p$ orbital (the moments are 3.46 and 3.06, respectively), leading to a greater bonding of the Ag^+ $5p$ orbital and the host CB states, and lowering the energy of the $5p$ bonding state relatively in the Ag^+ system. Combined with the greater antibonding of the $4d$ levels, the $nd \rightarrow (n+1)p$ transition in the Ag^+ system is much smaller relative to the free-ion transition than the like transition in the Cu^+ system.

Our results show very strong mixing of the Ag^+ $4d$ orbitals and the ligand orbitals in the impurity eigenfunctions with significant charge spreading to the ligand shell ($\sim 30\%$). In LiCl:Cu^+,[9] the corresponding Cu^+ $3d$ eigenfunctions show very little mixing of the Cu^+ $3d$ orbitals and the ligand $3p$ orbitals ($\sim 4\%$ in charge density). The strong mixing of the Ag^+ $4d$ orbitals and the ligand orbitals comes about, as mentioned above, because of the greater spatial extent of the Ag^+ $4d$ orbital as compared with the Cu^+ $3d$ orbitals. Another factor contributing to the mixing is the near degeneracy of the Ag^+ $4d$ energy levels with host-crystal VB states. The near degeneracy of the Ag^+ $4d$ orbitals with the VB can be understood by a simple argument. To zeroth order, the potential due to the host-crystal environment seen by the Ag^+ orbital is the Madelung potential. The Madelung potential is quite flat near the impurity site, and its effect on the energy lev-

els of Ag^+ is approximately a constant shift,[24] which for the case of LiCl is 0.360 a.u. The ionization potential for the free Ag^+ is 0.790 a.u. (Ref. 24). In the impurity system, the Ag^+ $4d$ energy is shifted by the Madelung potential to -0.430 a.u. The calculated host-crystal VB spans an energy range from -0.51 to -0.41 a.u., so that the shifted free-ion $4d$ level is predicted to lie in the VB. By contrast, the Cu^+ ionization potential is 0.743 a.u.; the shifted Cu^+ $3d$ level in LiCl:Cu^+ is therefore predicted to lie at -0.383 a.u., above the host-crystal VB. On the basis of this argument, then, we could expect to see strong mixing of the Ag^+ $4d$ and Cl^- $3p$ orbitals in LiCl:Ag^+ due to degeneracy of energy levels, whereas no such degeneracy-related mixing is expected for LiCl:Cu^+.

In our earlier work on NaCl:Cu^+ we generalized the bonding or antibonding argument used to explain the increase in the impurity $nd \rightarrow (n+1)s$ transition energy.[10] Assuming the impurity s-state energy level to be pushed up in energy, the $nd \rightarrow (n+1)s$ transition energy is increased whenever the energy of impurity d state is pushed up less. This occurs if the d states are more weakly antibonding as argued above, but also if the energy of the impurity d states is either unchanged or depressed relative to the free-ion levels, i.e., if the impurity d states are nonbonding or bonding. We applied this generalized argument to the NaCl:Cu^+ $nd \rightarrow (n+1)s$ transition, since the impurity $3d$ states in that system were found in the VB, and had no clear-cut bonding or antibonding character.

We can extend this reasoning to consider the implication for the crystal-field splitting of the impurity d states as the character of these states switches from antibonding to bonding. As a matter of geometry, the free-ion de_g orbitals have more spatial overlap with the E_g combination of ligand $3p$ orbitals than the dt_{2g} orbitals have with the corresponding T_{2g} combination. As a result, the energy shift due to bonding and antibonding is expected to be greater for the impurity de_g states. The same geometrical considerations are responsible for the splitting of the de_g and dt_{2g} levels due to the electrostatic field of the ions in the crystal but without the covalency effects. Because the e_g orbitals lie along the coordinate axes defined by the six negatively charged ligand ions, while the t_{2g} orbitals lie between these axes, the effect of the electrostatic field of the ligand ions is to raise the de_g levels relative to the dt_{2g}. We note that the magnitude of the crystal-field splitting seen in LiCl:Ag^+ (1.25 eV) is much greater than could be expected from the electrostatic consideration only.[25] The splitting of the $4d$ levels in this system thus clearly derives from the bonding or antibonding interaction discussed above. When the d levels lie above the VB, the antibonding shift of the energy levels enhances the electrostatic field splitting, since the de_g levels are shifted relatively higher by the antibonding than the dt_{2g}. If the d states are bonding, however, the situation is reversed, since the bonding then lowers the e_g levels relative to the t_{2g} levels, opposing the electrostatic field splitting. In such a case the crystal-field splitting is expected to be diminished or reversed.

KCl:Cu^+ is an example of a physical system to which these considerations may apply. In the series of related impurities, LiCl:Cu^+, NaCl:Cu^+, and KCl:Cu^+, the lattice spacing of the host crystal increases uniformly with the size of the cation. The Madelung shift of the Cu^+ $3d$ impurity levels thus decreases down the series, depressing the $3d$ levels relative to the VB. In LiCl:Cu^+, the SIC-LSD levels lie well above the VB, while in NaCl:Cu^+ they lie near the top of the VB. In KCl:Cu^+, the $3d$ levels can be expected to lie lower still, either toward the bottom or below the VB. The inversion of the crystal-field splitting due to the bonding of the impurity $3d$ levels may therefore be expected to be seen in the KCl:Cu^+ spectrum. Interestingly, two photon spectra, which distinguish the E_g from the T_{2g} transitions, show the conventional crystal-field splitting for the $de_g \rightarrow s$ and $dt_{2g} \rightarrow s$ bands in LiCl:Cu^+ and NaCl:Cu^+, whereas the two bands appear to fall at the same energy in KCl:Cu^+.[26]

B. Lattice relaxation

In this subsection we consider the question of lattice relaxation in the LiCl:Ag^+ system. Our calculation was carried out with the spacing between Ag^+ and its nearest-neighbor Cl^- ions, $d_{\text{Ag-Cl}}$, set equal to the host-crystal lattice spacing, $d_{\text{Li-Cl}}$. The free-ion radius of Ag^+ is 1.13 Å,[24] however, which is somewhat larger than the effective radius of Li^+ in LiCl, 0.94 Å,[24] and one intuitively expects the nearest-neighbor Cl^- ions to relax outward to accommodate the larger Ag^+ ion. Furthermore, the nearest-neighbor distance in AgCl, which has the same structure as LiCl, is 2.77 Å, compared to 2.57 Å for LiCl.

While these considerations suggest that some relaxation probably occurs in LiCl:Ag^+, the precise amount of the relaxation is unclear. We know of no experimental measurement for $d_{\text{Ag-Cl}}$. A value for $d_{\text{Ag-Cl}}$ was determined by Moine *et al.*[27] in their MS$X\alpha$ calculation of LiCl:Ag^+ using total-energy methods in conjunction with a model cluster approach (see Sec. IV D). They find a value of 3.23 Å for $d_{\text{Ag-Cl}}$, much larger than the host-crystal nearest-neighbor distance (2.57 Å) as well as the Ag-Cl distance in the AgCl crystal (2.77 Å). While this result shows the expected outward relaxation of the Cl^- ions, the magnitude of the calculated relaxation is larger than expected based on comparisons of the corresponding free-ion radii. The calculated relaxation, 0.66 Å, is much larger than the difference in the ionic radii for Ag^+ and Li^+ given above. This is true even when the *free-ion* value[24] for the Li^+ radius (0.68 Å) is used instead of the somewhat larger *effective* radius given above. Note that a similar calculation using the same method for NaCl:Cu^+ also predicts a significant outward relaxation of the Cl^- ions.[28] In that system, however, the relaxation is expected on physical grounds to be very small, since the Na^+ and Cu^+ free-ion radii are very similar, 0.98 and 0.96 Å, respectively. The model used in these calculations replaces the portion of the crystal outside the $AgCl_6$ cluster with an array of charges (see Sec. IV D). While this may be adequate for approximating the contribution of the

surrounding ions to the one-electron potential seen by the electrons in the $AgCl_6$ cluster, the model may not be appropriate for calculating lattice relaxation. Such a model does not include, for example, energy barriers to outward relaxation arising from the overlap of electronic charge clouds. Since we are not currently able with our SIC formalism to determine a self-consistent value for the lattice relaxation in LiCl:Ag^+, we adopt the host-crystal lattice spacing in our calculation.

How are we to view our results for LiCl:Ag^+ in light of the conclusion that some lattice relaxation is likely to occur? Let us first examine the qualitative effect that the neglect of lattice relaxation would have on our results. We have argued above that the greater overlap of the Ag^+ $4d$ and Cl^- $3p$ orbitals, compared to the overlap of analogous Cu^+ $3d$ and Cl^- $3p$ orbitals in NaCl:Cu^+, leads to a greater mixing between these orbitals in the eigenstates of the LiCl:Ag^+ impurity system, and a greater antibonding shift of the Ag^+ $4d$ impurity levels, relative to the corresponding shift of the Ag $5s$ level. Relaxing the Cl^- ions outward would tend to reduce the $4d$-$3p$ mixing, and thus the antibonding shift of the $4d$ levels, effectively increasing the $4d$-$5s$ transition energies. We do not expect the nearest-neighbor Cl^- ions to relax sufficiently to force a qualitative change in our analysis of the LiCl:Ag^+ spectrum. The outward relaxation of the ligand ions is opposed by forces due to the surrounding host-crystal ions. Since the energy difference between the $4de_g \rightarrow 5s$ and $4dt_{2g} \rightarrow 5s$ transitions is a measure of bonding or antibonding interaction between the impurity $4d$ and Cl-$3p$ orbitals, the large observed splitting (1.25 eV) as compared to the corresponding $3d$ splitting of 0.46 eV in LiCl:Cu^+ indicates that ligand-ion relaxation does not fully remove the increased overlap of the Ag^+-$4d$ and Cl-$3p$ orbitals in LiCl:Ag^+. While our calculations overestimate this splitting slightly (by 0.18 eV), this small difference suggests that our results provide a good description of host-impurity bonding in LiCl:Ag^+ despite our neglect of lattice relaxation.

It is possible, by comparing with the earlier NaCl:Cu^+ calculation,[10] to make a more quantitative estimate of the effect of neglecting relaxation on our results, and at the same time to explain why our results for LiCl:Ag^+ are in such good agreement with experiment, given that we have neglected relaxation. In the NaCl:Cu^+ SIC-LSD calculation we found the transition-energy results to *overestimate* the experimental transition energies by about 0.4 eV. We understood this overestimate to result from our use of the GSUO method for calculating the transition energies. The GSUO method does not account for orbital relaxation in the excited state (see Sec. II), thus effectively raising the upper state energy, and resulting in overestimates of the transition energy. We show in Ref. 10 how an improved technique which accounts for orbital relaxation and for the single-triplet splitting of the excited states can be used to give transition-energy results for NaCl:Cu^+ in good agreement with experiment. We expect that our calculated transition energies for LiCl:Ag^+ should overestimate the experimental results by roughly the same amount as seen in the NaCl:Cu^+ calculation. (The technique presented in Ref. 10 for calculating orbitally relaxed transition energies is not immediately applicable to the LiCl:Ag^+ transitions, because of the strongly mixed character of the eigenstates.) Since, as noted above, the effect of including lattice relaxation in our calculation would be to increase the transition energies, we believe that the effect of neglecting lattice relaxation is canceled by our neglect of orbital relaxation in calculating the transition energies.

C. Effect of the modified SIC-LSD treatment

In this calculation we modified the SIC-LSD algorithm applied previously to LiCl:Cu^+ and NaCl:Cu^+ to accommodate the multisite character of the impurity $4d$ states of LiCl:Ag^+. The original method[9] formulated for the Cu^+ impurities assumes the Cu^+ $3d$ eigenstates to be essentially identical to the SIC-LSD LO because of the very small admixture of the ligand valence orbitals. In LiCl:Ag^+, the strong impurity-ligand mixing gives the impurity $4d$ eigenstates a pronounced multisite character. Treating the impurity $4d$ states as SIC-LSD LO is a crude approximation, and a modified procedure was introduced in Sec. II B [Eqs. (25)–(27)]. To investigate the effect the cruder approximation would have on our results, we ran a separate SCF calculation using the earlier technique, i.e., assuming the impurity eigenstates to be SIC-LSD LO. For clarity, let us label the results of this test calculation "crude," whereas the results of our improved treatment shall be referred to as "refined." Using the GSUO approximation to determine the transition energies from the orbital energies, we find the $4de_g$ and $4dt_{2g}$ to $5s$ transition, respectively, to be 5.63 and 6.42 eV using the crude approximation. The $4de_g$ to $5p$ transition using the crude approximation is 7.26 eV. These results are all significantly smaller than the corresponding results using the refined approximation (6.01, 7.44, and 7.80 eV, respectively), and in much poorer agreement with experiment. It is easy to see why the crude approximation leads to smaller transition energies. Consider a simplified model of a transition between canonical orbitals in a multiatom system. Assume local orbitals ϕ_1 and ϕ_2 are related via a unitary transformation to the canonical orbitals ψ_A and ψ_B as in Eq. (9). The ψ's correspond in our LiCl:Ag^+ calculation to the mixed $4d$ impurity eigenstates, and the ϕ's to the corresponding atomiclike GWF. By our assumption that the ϕ's are the LO, we can write

$$U^{\mathrm{SIC}}\{\phi_1,\phi_2\} \leq U^{\mathrm{SIC}}\{\psi_A,\psi_B\} \ , \tag{28}$$

where $U^{\mathrm{SIC}}\{i,j\}$ is the self-interaction energy of orbitals i and j. Calculating the self-interaction according to the left-hand side of Eq. (29) is equivalent to our refined approximation, whereas the right-hand side is equivalent to the crude approximation. Now consider a transition from ψ_B to an excited canonical state ψ_C. If the density associated with the excited orbital is spread over a different region of space than ψ_A, then no transformation of ψ_A and ψ_C to more localized orbitals can be found, which leads to a significantly more negative U^{SIC}, and these orbitals can be taken to be the appropriate SIC LO for the excited configuration in both methods. The refined and crude methods would thus both find the same

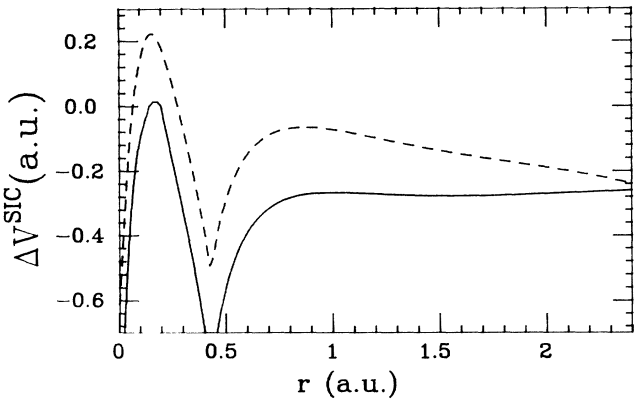

FIG. 3. Comparison of two SIC potentials for the Ag^+ 4*d* impurity states. The dashed curve is the potential calculated using the procedure of Ref. 10, which assumes highly localized impurity states. The solid curve is calculated using the refined procedure introduced in this work, which allows for the miltisite character of the impurity states in LiCl:Ag^+.

U^{SIC} for the excited state. The transition energy calculated by the refined method (as in our modified approach to LiCl:Ag^+) is thus larger than that of the crude method, because of the improved SIC treatment of the ground state. Shifting to a one-electron point of view, the SIC potential used for the impurity 4*d* states is relatively shallow in the crude approximation, when the multisite 4*d* eigenfunction is taken as a LO; in the refined treatment, on the other hand, the SIC potential for the impurity 4*d* state is essentially identical to the local V^{SIC} potential appropriate to the free-ion 4*d* orbital near the Ag^+ site, and to the V^{SIC} for the Cl^- 3*p* Wannier function near the Cl^- sites. This point is illustrated in Fig. 3 where both potentials are shown in the region around the Ag^+ ion. The content of Fig. 3 can be expressed in another way by considering the SIC contribution to the impurity 4*d* state orbital energy ($\langle \psi_{4d} | V_{4d}^{SIC} | \psi_{4d} \rangle$), calculated alternately using the two potentials shown in the figure. Using the V_{4d}^{SIC} potential based on the crude approximation, the SIC orbital energy contribution is −0.091 a.u., compared to a contribution of −0.190 a.u. for the refined method used in this work. For reference, the SIC shift of the free-ion Ag^+ 4*d* orbital energy is −0.200 a.u., and it can thus be seen that the refined SIC-LSD treatment restores SIC energy lost by treating the multisite 4*d* eigenfunction as a LO.

D. Comparison with other theoretical results

Moine *et al.*[27] have also studied the LiCl:Ag^+ system, using a model cluster multiple-scattering $X\alpha$ (MS $X\alpha$) technique of Slater and Johnson.[29] Their model cluster procedure places spheres on the impurity site and the six sites of the first-nearest-neighbor shell. A different exchange parameter α is used inside the Ag^+ and Cl^- spheres, respectively, each taken from Schwarz's tabulation.[30] The $AgCl_6^{-5}$ cluster is surrounded by an array of charges to mimic the effect of the host-crystal environment. Transition energies are calculated using Slater's transition states method. We use the average of the singlet and triplet transition energies of the MS $X\alpha$ calculation of Ref. 27 for comparison with the SIC-LSD results. The MS $X\alpha$ work gives $4de_g \rightarrow 5s$ and $4dt_{2g} \rightarrow 5s$ transition energies, respectively, as 4.04 and 4.71 eV for $d_{Ag\text{-}Cl} = 6.20$ a.u., and as 6.58 and 7.87 eV for $d_{Ag\text{-}Cl} = 5.20$ a.u. The latter set is closer to our SIC-LSD results, which corresponds to $d_{Ag\text{-}Cl} = 4.86$ a.u. In view of the sensitivity of MS $X\alpha$ transition energies to the value of $d_{Ag\text{-}Cl}$, it is difficult to draw instructive conclusions from this comparison.

The MS $X\alpha$ calculation shows the Ag^+ 4*d* impurity states to have a more metallic character in the gound state than the antibonding 4*d* states have in the SIC-LSD calculation. The MS $X\alpha$ states (for $d_{Ag\text{-}Cl} = 6.20$ a.u.) are reported to be 82% and 92% localized on the Ag^+ site, whereas the comparable figures for the SIC-LSD calculation are 62% and 73%, respectively, for the $4de_g$ and $4dt_{2g}$ states. Their excited a_{1g} state, which corresponds to our 5*s* state, is poorly localized in the MS $X\alpha$ calculation. Only 13% of the 5*s* charge is associated with Ag^+. The authors also report a delocalized excited state lying at slightly lower energy than the 5*s*. As mentioned above, the Mulliken analysis for the 5*s* state in the SIC-LSD calculation cannot be taken as completely reliable because of significant overlap of the long-range basis functions centered on different sites. Approximate population numbers for the SIC-LSD 5*s* state can, however, be obtained by removing some of the long-range functions from the basis. Removing the longest-range SGO's on the Ag^+ and the ligand sites, the population numbers for the SIC-LSD 5*s* are 33% Ag^+ and 67% ligand, indicating a somewhat more localized 5*s* state than is seen in the MS $X\alpha$ work. No delocalized excited state is found in our calculation lying below the 5*s*.

The MS $X\alpha$ calculation examines only results for the impurity $d \rightarrow s$ transition. The two-shell cluster model used in the MS $X\alpha$ work is not consistent with the more extensive charge distribution of the 5*p* state.

V. CONCLUSIONS

We have presented above the results of a self-consistent SIC-LSD calculation of the electronic structure of LiCl:Ag^+, using a Gaussian-based LCAO method. The one-electron states associated with the impurity ion were found to be strongly mixed combinations of impurity- and host-crystal orbitals. The multisite character of these states motivated us to modify the approximate method for deriving the SIC potential developed in earlier work[9,10] on Cu^+ impurities in which the impurity states are sufficiently atomiclike to be taken as the LO's for SIC. The modified method defines an approximate and computationally efficient self-interaction correction for the multisite impurity states, based on the general SIC-LSD formalism. The SIC potential has a density-weighted form, and a multisite character similar to that of the impurity states. With the refined SIC-LSD method we calculated the energies of the $4d \rightarrow 5s$ and $4d \rightarrow 5p$ impurity transitions. Our results, shown in Table I, are in

very good agreement with experiment,[13] and lead to the identification of the absorption band at 8.0 eV as the $4d_{eg} \rightarrow 5p$ transition.

The SIC-LSD procedure used in this work is computationally efficient and easy to implement. It is based on the identification of approximate SIC-LSD LO, and the use of a density-weighted expression for the SIC potentials associated with the canonical one-electron states (see Sec. II). It remains a problem to calculate total energies for many-atom systems with the SIC-LSD theory. A total-energy option would allow the use of SIC-LSD for determining structural properties; for example, the lattice relaxation of the ligand ions in response to the presence of the Ag^+ impurity in LiCl:Ag^+. It would be of particular interest to use SIC-LSD to calculate total energies for systems in which the energy-level structure is qualitatively different in SIC-LSD than in LSD. In LiCl:Ag^+, for example, the impurity $4d$ bands are degenerate with the host-crystal valence band in SIC-LSD, whereas in LSD they lie somewhat above the valence levels. Such differences in the electronic structure may lead to distinct differences in the structural properties calculated in SIC-LSD versus LSD.

ACKNOWLEDGMENTS

It is a pleasure to acknowledge the enlightening comments offered by Professor D. S. McClure in connection with the interpretation of the experimental data. We are grateful for many discussions of this work with Dr. S. C. Erwin, Dr. R. A. Heaton, and Dr. M. R. Pederson. This work was supported by National Science Foundation Grant No. DMR-85-00488.

*Present address: Complex Systems Theory Branch (Code 4692), Condensed Matter and Radiation Sciences Division, Naval Research Laboratory, Washington, D.C. 20375-5000.

[1]P. Hohenberg and W. Kohn, Phys. Rev. **136**, B864 (1964).
[2]W. Kohn and L. J. Sham, Phys. Rev. **140**, A1133 (1965).
[3]O. Gunnarsson and B. I. Lundquist, Phys. Rev. B **13**, 4274 (1976).
[4]M. L. Cohen, Phys. Scr. T **1**, 5 (1982), and references therein.
[5]J. P. Perdew and A. Zunger, Phys. Rev. B **23**, 5048 (1981).
[6]J. G. Harrison, R. A. Heaton, and C. C. Lin, J. Phys. B **16**, 2079 (1983).
[7]R. A. Heaton and C. C. Lin, J. Phys. C **17**, 1853 (1984).
[8]S. C. Erwin and C. C. Lin, J. Phys. C **21**, 4285 (1988).
[9]R. A. Heaton, J. G. Harrison, and C. C. Lin, Phys. Rev. B **31**, 1077 (1985).
[10]K. A. Jackson and C. C. Lin, Phys. Rev. B **38**, 12 171 (1988).
[11]S. C. Erwin and C. C. Lin, Phys. Rev. B **40**, 1892 (1989).
[12]M. R. Pederson and B. M. Klein, Phys. Rev. B **37**, 10 319 (1988).
[13]C. Pedrini, J. Phys. Chem. Solids **41**, 653 (1980).
[14]C. Pedrini, Phys. Status Solidi B **87**, 273 (1978).
[15]M. R. Pederson, R. A. Heaton, and C. C. Lin, J. Chem. Phys. **80**, 1972 (1984).
[16]M. R. Pederson, R. A. Heaton, and C. C. Lin, J. Chem. Phys. **82**, 2688 (1985).
[17]W. Kohn and J. R. Onffroy, Phys. Rev. B **8**, 2485 (1973).
[18]W. P. Menzel, K. Mednick, C. C. Lin, and C. F. Dorman, J. Chem. Phys. **63**, 4708 (1975).
[19]G. Baldini and B. Bossachi, Phys. Status Solidi **38**, 325 (1970).
[20]H. Benschop, Y. N. Joshi, and Th. A. M. Vankleef, Can. J. Phys. **53**, 700 (1975).
[21]R. S. Mulliken, J. Chem. Phys. **23**, 1833 (1955); **23**, 1841 (1955).
[22]J. G. Harrison and C. C. Lin, Phys. Rev. B **23**, 3894 (1981).
[23]C. Pedrini, H. Chermette, A. B. Goldberg, D. S. McClure, and B. Moine, Phys. Status Solidi B **120**, 753 (1983).
[24]C. Kittel, *Introduction to Solid State Physics, 5th ed.* (Wiley, New York, 1976).
[25]S. Nagasaka, J. Phys. Soc. Jpn. **50**, 1570 (1981).
[26]S. A. Payne, A. B. Goldberg, and D. S. McClure, J. Chem. Phys. **81**, 1529 (1984).
[27]B. Moine, H. Chermette, and C. Pedrini, J. Chem. Phys. **85**, 2784 (1986).
[28]H. Chermette and C. Pedrini, J. Chem. Phys. **77**, 2460 (1982); **75**, 1869 (1981).
[29]J. C. Slater, *The Self-Consistent Field for Molecules and Solids* (McGraw-Hill, New York, 1974).
[30]K. Schwarz, Phys. Rev. B **5**, 2466 (1972).